Progress Report for the IN2P3 Scientific Council, June 24-25, 2024

# Improved Search for Tensor Interactions in Nuclear Beta Decay

(*bSTILED* : **b**: **S**earch for **T**ensor **I**nteractions in nuc**L**ear b**E**ta **D**ecay)

Xavier Fléchard[a] and Oscar Naviliat-Cuncic[b,c]
for the bSTILED collaboration[1]

[a] Université de Caen Normandie, ENSICAEN, CNRS/IN2P3, LPC Caen UMR6534
F-14000 Caen, France
[b] Facility for Rare Isotope Beams and Department of Physics and Astronomy, Michigan State University,
East Lansing, MI 48824, USA
[c] International Research Laboratory for Nuclear Physics and Nuclear Astrophysics, CNRS-MSU,
East Lansing, MI 48824, USA

(May 23, 2024)

## 1. Summary

The goal of the *bSTILED* project is to search for signatures of New Physics (NP) which would manifest themselves through phenomenological tensor couplings in nuclear beta decay. More specifically, this search is sensitive to tensor couplings involving left-handed neutrinos. The most sensitive parameter to probe such couplings is the Fierz interference term and the most direct way to determine this parameter is through a measurement of the beta-particle energy spectrum. A high precision measurement of the entire beta-particle energy spectrum requires a very careful selection of the candidate such that the theoretical description of the spectrum, including "Standard Model backgrounds" is well under control and does not hamper the sensitivity goal. Also, the decay should display a number of properties such as to perform a clean measurement within a reasonable time.

The *bSTILED* project was proposed to-- and funded by the French National Research Agency (ANR) in 2020. It is a collaboration between three French institutions: the Laboratoire de Physique Corpusculaire de Caen (LPC Caen), the Grand Accélérateur National d'Ions Lourds (GANIL), and the Laboratoire National Henri Becquerel (LNHB) from CEA.

The *bSTILED* project aims reaching the highest ever possible level of sensitivity to measure the Fierz interference term in a Gamow-Teller transition and the selected candidate is the decay of $^{6}$He. To this end, the project has implemented an improved calorimetry technique using implanted radioactive beams to achieve a geometry such that the major instrumental effect (i.e. electron backscattering) is totally eliminated. The project was organized in two phases. Within Phase I, two experiments have been carried out at GANIL, one with a low-energy beam (25 keV kinetic energy) and the other with a high-energy beam (312 MeV kinetic energy). The data analysis of the two experiments is in progress and should each produce single-experiment competitive constraints on tensor couplings.

---

[1] G. Craveiro (LNHB), X. Fléchard (LPC Caen), R. Garreau (LPC Caen), L. Hayen (LPC Caen), T.E. Haugen (MSU), M. Kanafani (LPC Caen), S. Leblond (LNHB), E. Liénard (LPC Caen), X. Mougeot (LNHB), O. Naviliat-Cuncic (MSU & IRL NPA), J.C. Thomas (GANIL).

Phase II of the project relies on a careful evaluation of the pros and cons of the two techniques, to possibly reach a level of sensitivity which would be competitive with constraints from LHC. This requires a detailed analysis of systematic and instrumental effects of both experiments, a task that is being started in 2024 along with the data analysis of the measurement carried out with the high-energy beam.

As indicated above, the main goal of the project is the search for exotic tensor type interactions possibly contributing to beta decay. Among the "Science Drivers" within the national long range plan exercise, this project is embedded within the *Searches for Unknown Particles and Interactions (New Phenomena).* The current state-of-the-art and the projected scientific impact are described below.

## 2. Scientific Context and State of the Art

Despite the impressive successes of the Standard electroweak Model (SM) there are cosmological observations and theoretical reasons to believe that it is actually part of a larger theoretical framework. Searches for signatures of NP beyond the SM are commonly carried out at three main frontiers, without sharp borders: the high-energy frontier, the cosmological frontier and the high precision frontier. The high-energy frontier directly explores new energy domains with powerful particle colliders like the Large Hadron Collider (LHC) at CERN. The cosmological frontier includes searches for anti-matter in the universe, probing the cosmic microwave background as well as indirect searches for dark matter. The high precision frontier (or "intensity frontier") involves mainly precision measurements at low energies, over a broad range of physical systems, from molecules up to elementary particles. The ultimate goal of these efforts is to detect a signature of NP and to provide inputs for the development of a "new Standard Model" of nature's fundamental interactions.

It has been useful to sort the different low energy probes into three main categories, in terms of their discovery potential [Cir13]: (a) rare and forbidden decays; (b) precision tests; and (c) cosmological and astrophysical probes. The precision tests category includes in turn the study of neutral-current processes and of charged-current processes. The present proposal belongs to this last category and more specifically to the sector of semi-leptonic weak processes involving the lightest quarks.

With the assumption that the NP originates at some very high-energy scale, one can consider the SM as a low-energy limit of a more fundamental theory. This is comparable to Fermi's theory of nuclear beta decay, which is an effective low-energy limit of the fundamental description of a semi-leptonic process within the SM involving the exchange of the charged weak boson. In the absence of signatures of NP, it has been convenient to describe the dynamics below the energy scale $\Lambda$ at which new particles would appear, through an effective field theory (EFT) in which the possible new heavy particles affect the dynamics through higher dimensional operators [Cir13]. The advantage of this approach is not only that it is general but also that it is efficient. The data analysis can be done once for all experimental inputs, and its outcome can be applied to any specific scenario beyond the SM. This EFT framework enables furthermore comparing, in a general way, the NP sensitivity among different low-energy probes but also relative to other searches, such as those performed at the LHC.

The constraints on NP obtained from nuclear and neutron decay experiments have

regularly been updated in the past [Vos15, Gon19, Fal21]. These analyses make the connection between the traditional Lee and Yang parametrization of the beta-decay Hamiltonian, which uses couplings at the nucleon level [Jac57], with the EFT parametrization at the quark level in terms of Wilson coefficients. The relations between the two, which involve the hadronic charges, can for instance be found in Ref. [Gon19]. The most general formulation consistent with Lorentz invariance involves 20 independent real parameters (10 complex coupling constants) which can be reduced under some assumptions. The assumption of time-reversal invariance in the light-quark sector imposes all couplings to be real. Next, since the interference between the terms involving right-handed neutrinos and the SM are suppressed, they are sometimes neglected when analyzing data from nuclear and neutron decays. Under such an approximation, the number of Wilson coefficients associated with NP is reduced to four [Gon19], noted $\epsilon_R$, $\epsilon_S$, $\epsilon_T$, and $\epsilon_P$, plus an overall normalization, $\tilde{V}_{ud}$. Finally, beta-decay correlation measurements are most sensitive to Wilson coefficients $\epsilon_S$, and $\epsilon_T$, which drive phenomenological scalar and tensor terms in the Hamiltonian, involving left-handed neutrinos.

The constraints obtained from these experiments have been compared with other sensitive probes at low energies, such as pion decay, as well as to the then state-of-the-art and future constraints from the LHC. The left panel on Fig.1 shows the 90% CL constraints obtained on $\epsilon_S$ and $\epsilon_T$ from the analysis of Ref. [Gon19], which were available when this project started in 2020. The green horizontal band shows the constraint on $\epsilon_S$ extracted from the energy integrated Fierz term contributing to $\mathcal{F}t$–values of superallowed $0^+ \rightarrow 0^+$ pure-Fermi transitions [Har15], which provide the most sensitive probe of $\epsilon_S$. The survey of pure-Fermi transitions published in 2020 [Har20] did not modify those constraints in any significant way. The orange vertical band on the left panel on Fig.1 shows the constraint on $\epsilon_T$ obtained from radiative pion decay, which constitutes the most sensitive low energy probe of $\epsilon_T$ from a single experiment. The blue circle shows the constraints extracted from the analysis of the channel $pp \rightarrow e + \text{MET} + X$ at the LHC (CMS data), where MET denotes the missing transverse energy. This was obtained by comparing the absence of events in the cross section, for a transverse energy larger than 1.5 TeV, with respect to the expected SM background, at a center of mass energy of 8 TeV and an integrated luminosity of 20 fb$^{-1}$. The black ellipse provides the combined constraints on the two coefficients obtained from all beta-decay data. It includes the data from the $\mathcal{F}t$–values of superallowed pure-Fermi transitions and in particular the neutron lifetime and the electron-decay asymmetry from neutron decay. It is interesting to observe the competition between the low energy and the LHC results. This competition persisted in a new analysis of beta-decay data, which added results from nuclear mirrors transitions and updated two channels from the LHC, as shown in Fig.2 [Fal21].

Run 3 at LHC is expected to last until 2026, at a center of mass energy of 13.6 TeV and with a total integrated luminosity of about 500 fb$^{-1}$. Assuming no signal of NP is seen, the constraints obtained from direct searches of new particles through the channel discussed above, $pp \rightarrow e + \text{MET} + X$, are shown by the dashed blue line on the right panel of Fig.1 [Gon19]. This analysis assumed a total integrated luminosity of about 300 fb$^{-1}$. On the vertical scale, the width of this constraint is comparable to the current one obtained from the $\mathcal{F}t$-values, but the constraint on the tensor coefficient will be significantly improved.

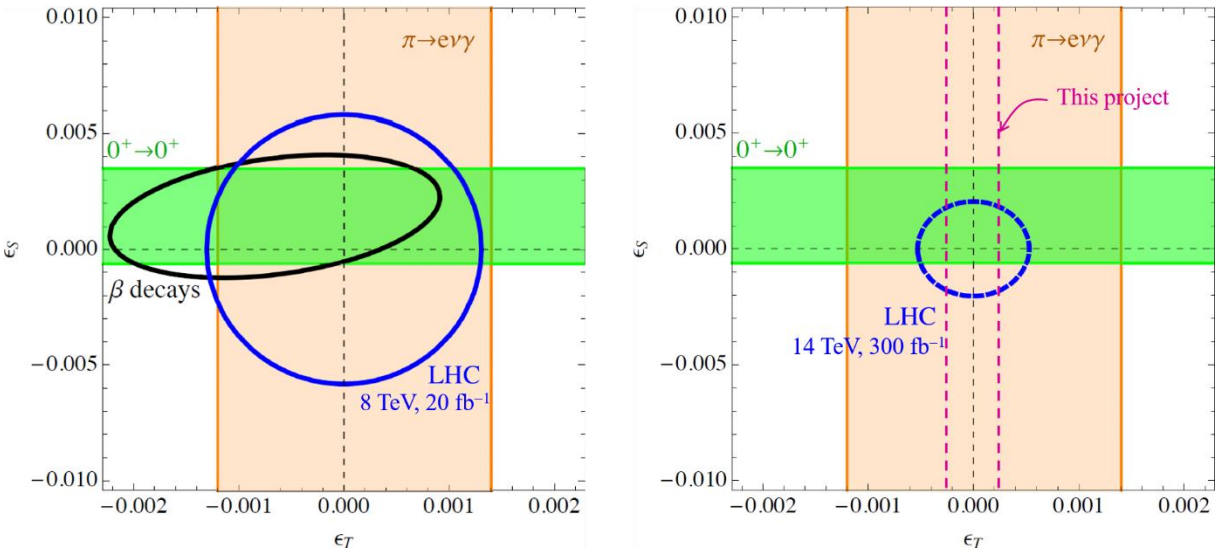


Fig.1. 90% CL constrains on the scalar and tensor coefficients from semi-leptonic decays and from the LHC. Left panel: constraints when the project was started (from [Gon19]). Right panel: the dotted lines indicate the projected sensitivities from the LHC (blue) and from this proposal (magenta) (adapted from [Gon19]).

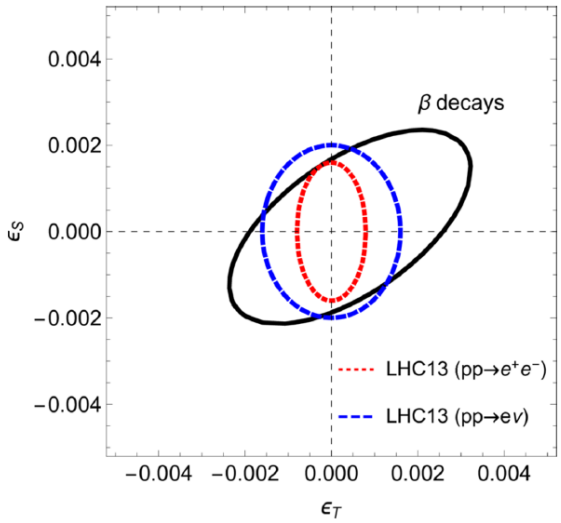


Fig.2. 90% CL constrains on the scalar and tensor coefficients obtained from beta-decay data and from two channels at the LHC [Fal21]. We stress that the tensor coefficient here has been normalized by a factor 1/4 compared to the parameterization used in Fig.1.

The global analysis performed in Refs. [Gon19, Fal21] confirmed the observations made earlier [Bha12, Nav13] concerning the sensitivity of different beta-decay correlations. For couplings involving left-handed neutrinos, the most sensitive and promising observable to improve the constraint on tensor couplings from beta decay is the Fierz interference term, noted $b$ [Jac57], in a pure Gamow-Teller (GT) transition, because of its linear dependence on exotic couplings through interferences with the SM vector and axial-vector ones.

A number of results in beta decay were published during or after the global analyses presented above. These are summarized here and do not significantly change the constraints due to their moderate statistical or systematic uncertainties. In neutron decay, the analyses of the differential beta-decay asymmetry yielded the value $b_n = 0.017 \pm 0.021$ for the PERKEO collaboration [Sau20], and $b_n = 0.066 \pm 0.041_{\text{stat}} \pm 0.024_{\text{syst}}$, for the UCNA collaboration [Sun20]. A reanalysis of the beta-neutrino angular correlation

data by the aSPECT collaboration resulted in $b_n = -0.0098 \pm 0.0193$ [Bec24], reaching a slightly improved precision than PERKEO. In nuclear decays, there have been several measurements of the recoiling nucleus spectrum in Gamow-Teller transitions to deduce the beta-neutrino angular correlation: in $^{32}$Ar decay [Ara20], in $^{6}$He decay [Mul22], and in the mass $A$=8 system [Lon24]. None of these results sets competitive constraints on tensor couplings involving left-handed neutrinos.

## 3. Description of the Project

The Fierz term enters the expression of the energy spectrum through a factor $(1 + bm/E)$, where $m$ is the electron mass and $E$ is the beta-particle total energy. In a pure GT transition, the relationship between the Fierz term and the tensor coefficient in the parameterization of Ref. [Gon19], is simply given by $b_{GT} = 6.2\epsilon_T$ where the tensor hadronic charge, $g_T$, has been used [Gon19].

The ultimate precision goal of this project is to reach a total uncertainty $\Delta b_{GT} = 1 \times 10^{-3}$ at 1σ, with statistical and systematic contributions of comparable magnitudes. In the absence of a signal from NP, this corresponds to the 90% CL constraints shown by the vertical dashed magenta lines on the right panel of Fig.1. Compared to constraints from radiative pion decay, this would represent an improvement by a factor of 5 whereas it would provide a factor of about 2 improved constraints compared with the projected sensitivities of the LHC 14 TeV, 300 fb$^{-1}$.

### 3.1 Criteria for the selection of a candidate

The selection of a candidate for a measurement of the full beta-energy spectrum in a GT transition requires the careful analysis of a number of theoretical and experimental aspects. On the theoretical side, the SM description of the spectrum shape must be performed with an accuracy that does not hamper the precision goal. This applies to all terms entering the description of the shape, including the Coulomb, radiative as well as hadronic corrections. On the experimental side, the decay scheme must be as simple and clean as possible, with a nuclear lifetime enabling the collection of the required statistics within a reasonable time.

Some of the criteria in the selection of an ideal candidate transition include:

- The choice of a pure transition (in contrast to a mixed transition) which eliminates the determination of the mixing ratio between the Fermi and Gamow-Teller matrix elements and also enables to strictly constraint the tensor coefficient without correlation with the scalar one.
- For allowed transitions, the description of the shape is, to first order, independent of the dominant nuclear matrix element, which drives the total decay rate. This matrix element enters as an overall factor of the spectrum shape.
- In order to limit the effect of Coulomb corrections, the transition must have a relatively high energy, of a few MeV, whereas the daughter nucleus must also have a low atomic number.
- Corrections to the hadronic weak current enter at recoil order through the effect of induced weak form factors and the dominant term is the weak magnetism form factor. For GT transitions within an isospin triplet it is possible to accurately determine this form factor using the so-called "strong form" of the principle of Conservation of the Vector Current [Gel58]. This relates the strength of the weak decays within a triplet to the strength of the iso-vector M1 transition from the isobaric analogue $T_3 = 0$ state (Fig.3, middle panel). Another form factor of the hadronic weak current is the induced

tensor and it is suitable this be either small or accurately known.

• The analysis of the kinematic sensitivity as a function of the end-point energy [Gon16] showed that the optimal value is about twice the electron mass. It also showed that the neutron and $^6$He decays have very comparable sensitivities provided the measurements use a threshold at 5% relative to the end-point energy, a condition that is more difficult to achieve for low end-point energies.

• It is preferable the transition take place to the ground state of the daughter nucleus, without the presence of additional de-excitation γ rays. Electron decays are also preferred over positron decays to avoid the presence of 511 keV annihilation photons.

With all the criteria above, it appears that the beta decay of $^6$He (3.5 MeV endpoint, $T_{1/2}$ = 0.8 s) nicely fulfils all requirements and makes $^6$He the ideal candidate for the measurement of the beta-energy spectrum [Nav16]. Figure 3 shows the most relevant information concerning $^6$He. The corrections to the phase space of this allowed transition are expressed as factors of the form $[1 + \eta(T_e)]$, and the energy dependent functions $\eta(T_e)$ are plotted on the right panel of Fig.3. Table I lists all the experimental inputs that enter the description of the energy spectrum. The uncertainty on each of these quantities produces a systematic uncertainty on $b_{GT}$ that is quoted in the second column. The largest of them is due to the weak magnetism form factor, which dominates the total theoretical uncertainty. This last is sufficiently well known to reach the precision goal of the present project.

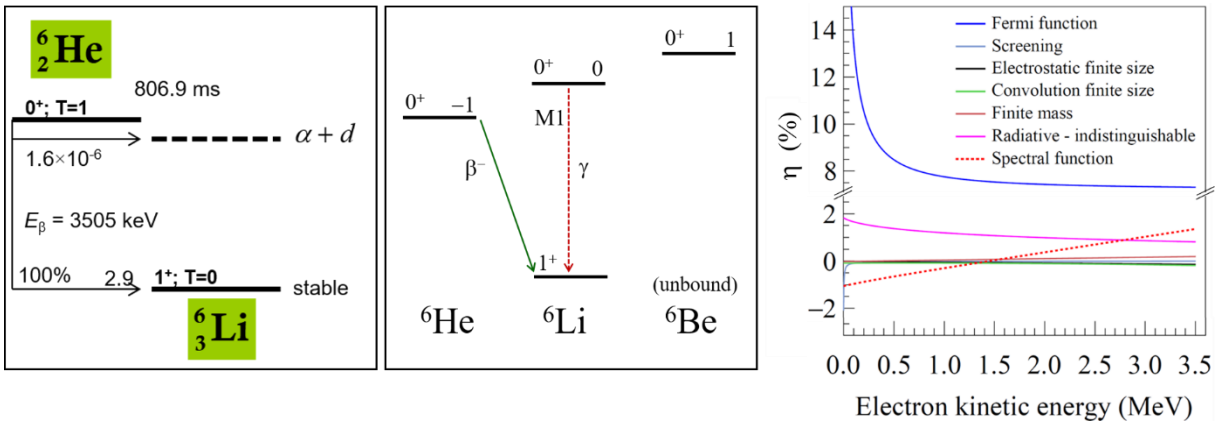


Fig.3. Left panel: scheme of the $^6$He beta decay. Middle panel: isospin-triplet for mass $A$=6. The weak magnetism form factor in $^6$He decay can be extracted from the width of the M1 analogue transition in $^6$Li. Right panel: corrections to the phase space for the description of the energy spectrum. The contribution of induced weak currents is labelled "Spectral function" (adapted from Ref. [Huy19]).

| **Source** | $\Delta b_{GT}$ |
|---|---|
| Nuclear charge radius of $^6$Li | $4.6\times10^{-5}$ |
| End-point energy of the transition | $1.8\times10^{-4}$ |
| Weak magnetism form factor | $5.7\times10^{-4}$ |
| Induced tensor form factor | $1.9\times10^{-5}$ |
| **Total theoretical uncertainty** | $\mathbf{6.0\times10^{-4}}$ |

Table I. Experimental properties that enter the theoretical description of the beta-energy spectrum along with the systematic uncertainty they produce on the extracted Fierz term. The first line comes from Ref. [Huy20].

### 3.2 Measuring principle and improvements

The major instrumental limitation preventing reaching an uncertainty below $1 \times 10^{-2}$ on the Fierz term from a measurement of the beta-energy spectrum is the backscattering of electrons from detectors. This effect has been extensively studied with various simulation

codes in the energy range of experiments in nuclear and neutron beta decays [Mar03, Mar06, Gol08, Sot13] and compared with experimental data. The differences between results obtained with different codes and experiments have enabled to conclude that the reliability and accuracy in the description of backscattering is not sufficiently high to meet the required level of precision. This has motivated the implementation of new calorimetry techniques using radioactive beams [Nav16], based on the $4\pi$ detection of beta particles, to eliminate the effect of backscattering.

Two earlier measurements implementing a calorimetry technique have been performed at the National Superconducting Cyclotron Laboratory (NSCL) at Michigan State University, using fast beams of $^{6}$He (47 MeV/nucleon) and $^{20}$F (132 MeV/nucleon) implanted deep into CsI(Na) detectors such as to realize a calorimetric configuration for beta particles with several MeV energies. The description of these experiments can be found in Refs. [Huy19, Hug19]. An instrumental effect that remains when detecting electrons slowing down in matter is the partial energy loss through Bremsstrahlung radiation that can escape the detector. For the conditions of the $^{6}$He measurement at NSCL, an upper limit on this geometry dependent effect has been obtained through Geant4 simulations [Huy18].

The *bSTILED* project reported here, proposed in a first phase (Phase I), two measurements of the beta-particle energy spectrum implementing the calorimetric techniques using both, fast (52 MeV/nucleon) and slow (25 keV kinetic energy) radioactive ion beams from GANIL. The interest in using very different beam energies resides in the associated background and/or instrumental effects. Whereas a fast ion beam produces a well-localized small source fully surrounded by the active material of the detector, with negligible diffusion, the beam produces reactions during slowing down and so the associated background. For illustration, in the measurement performed at NSCL with $^{6}$He implanted on CsI(Na), the level of beam-induced background was comparable to that of the ambient background [Huy19] and produced the third largest systematic effect. This is however dependent on the detector material. In contrast, with the low-energy beam, the ions are implanted within a few hundred of nm from the detector surface, without producing any additional background. However, the realization of a full $4\pi$ geometry at low energy becomes more involved and the problem of diffusion/effusion requires some attention. In addition, several other improvements of the technique have been implemented compared to the exploratory measurements performed at NSCL.

A first improvement of *bSTILED* is the use of YAP(Ce) inorganic scintillators [Mos98] for the detection of beta particles and the measurement of their energy. The selection of YAP resulted from a compromise between fast response, acceptable energy resolution as well as the best differential linearity over the largest possible energy range. In addition, Monte-Carlo simulations have shown that the distortion of the beta-energy spectrum due to escaping Bremsstrahlung radiation is a factor of about 2 smaller for YAP than for CsI for crystals of the same shape [Kan23b]. A second improvement was the use of a hollow plastic scintillator (PVT) cylinder surrounding the YAP crystal in a phoswich configuration (Fig.4, left panel). Each detector is equipped with an external $^{241}$Am source located on the side of the PVT. By implementing a pulse-shape discrimination scheme (Fig.4, right panel), such configuration allows monitoring the stability of the system and the correction of rate dependent effects using the signals from the $^{241}$Am source.

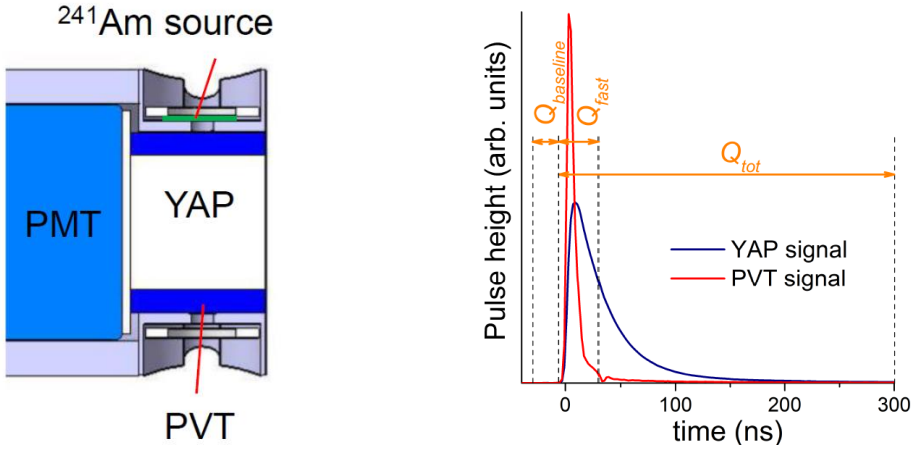


Fig.4. Left: Phoswich configuration of the YAP scintillator surrounded by a hollow PVT cylinder. Both scintillators are readout by a single photomultiplier. Right: time windows for the implementation of a pulse-shape discrimination technique on the signals from the YAP and PVT (from Ref. [Kan22]).

Another improvement is related to the use of the FASTER real-time data acquisition system, developed at LPC Caen. The system enables the definition of four independent charge integration windows for each signal, avoiding having to record the waveforms. In particular, one of the windows can be defined up to –30 ns before the trigger time, enabling the integration of the signal baseline (Fig.4, right panel). This is important for the determination of the calibration offset.

### 3.3 Radioactive source developments

Within the *bSTILED* project, the LNHB is in charge of developing calibration sources to accurately characterize the response functions of detectors. Following developments made for the measurement of $^{14}$C and $^{204}$Tl beta spectra [Sin23], sources will be made by depositing a drop of radioactive solution on an ultra-thin Mylar® film (500 nm thick) stretched over a support ring. The sources will then be freeze-dried before sealing with a second, identical film to avoid radioactive contamination of the detectors. The mother radioactive solutions will first be characterized at LNHB by gamma spectrometry to accurately quantify the possible presence of contaminating radionuclides. Since LPC Caen has not the necessary authorizations to host these sources (formally considered unsealed), the calibration of the detectors will be carried out at LNHB. The initial list of useful radionuclides for the project included $^{90}$Y/$^{90}$Sr, $^{89}$Sr and $^{32}$P, but other radionuclides have since then been identified. This follows a recent theoretical and experimental analysis of the beta decay of $^{99}$Tc measured with very high precision using magnetic metal calorimeters [Pau23].

To ensure the best possible accuracy, these calibration sources must be used in the closest configuration than the actual measurements, for example clamped between the two detectors used for the low-energy experiment (see below). The source support must therefore be larger than the diameter of the detectors (about 70 mm) and must be easy to attach to the detectors. As the usual sources produced at LNHB have a significantly smaller diameter (15 mm), additional developments will be required to adapt two critical instruments (the freeze-dryer and the electro-sprayer) to the dimensions of the source supports.

### 3.4 Scientific production

A first by-product of the *bSTILED* project, obtained from the measurement performed with the low-energy beam at GANIL (see below) is the most precise determination of the $^{6}$He half-life [Kan22], resolving thereby a longstanding discrepancy between two sets of precision data. This also led to a new nuclear data evaluation for this nucleus carried out by Xavier Mougeot within the International Decay Data Evaluation Project collaboration [Mou22].

The analysis of the data from the low energy beam experiment was presented at conferences [Kan23a] and was the main topic of the PhD thesis of Mohamad Kanafani [Kan23b]. Graduate student Gaël Craveiro is working at LNHB on redesigning the electronics of the beta-spectrometer device to minimize the noise, and has also developed a new spectral deconvolution approach [Cra24].

Other by products of the project, which are in the queue for publication are: 1) the benchmark of Geant4 simulation for the description of the Bremsstrahlung escape radiation, determined with the MTAS detector at FRIB (see below); 2) the detailed quantification of the backscattered fraction using the data from the low-energy experiment. Although this is not necessary for the measurement of the Fierz term, it will provide useful data to improve the description of electron backscattering (see below); 3) A new and more accurate description of the YAP response function using radioactive sources.

## 4. Genesis and Time Line

The *bSTILED* project is a collaborative effort between three French institutions which share their expertise on critical aspects related to the project. These include: i) the production of the suitable beta emitter, $^{6}$He, at the appropriate energies and with sufficient intensities and purities (GANIL); ii) the design, construction and characterization of the detectors, the adaption of the digital data acquisition system for the measurements, the data analysis and the assessment of systematic effects (LPC Caen); and iii) the production of calibration sources and the study of additional minute effects that contribute to the beta energy spectrum and which are relevant for the shape analysis (LNHB). Since the necessary expertise is available within a handful group of French laboratories, there was no need to involve international collaborators.

The project was proposed in 2020 to the French National Research Agency within the General Call. It was approved for funding and, after an extension, the contact will end in March 2026. In parallel, the proposal to perform both experiments was submitted in 2020 to the GANIL Program Advisory Committee, and was approved with high priority. Besides the labor support from CNRS for personnel at LPC Caen and GANIL, to assist in different aspects of the preparation and running of experiments, as well as for a PhD thesis that started in 2023, the *bSTILED* project did not request any additional funding from IN2P3 for equipment or maintenance.

From its inception, the project was conceived in two "Phases". The goal of Phase-I is to reach a precision of $\Delta b_{GT} = 4 \times 10^{-3}$ at 1σ on the Fierz term, with statistical and systematic contributions of comparable magnitudes. This level of precision is dictated by the benchmark sensitivities obtained from the global analysis in Ref. [Gon19, Table 8]. It is the precision that has to be reached on $b_{GT}$ in order for this parameter to be actually sensitive in constraining exotic couplings from beta decay. Achieving this precision will in

fact provide the tightest constraint on tensor couplings from a single low-energy probe. It will also enable the validation of the control of instrumental effects. Phase I is composed of two "Steps", associated with the two experiments performed at GANIL. After completion of the data analysis, the details of the two experiments will be evaluated in terms of possible improvements to be implemented for Phase II, with the final goal to reach a precision of $\Delta b_{GT} = 1 \times 10^{-3}$.

### 4.1 Phase I – Step 1: low energy experiment at LIRAT/GANIL

A noticeable landmark of Step 1 within Phase I was achieved by performing the experiment for the measurement of the beta-energy spectrum with the low energy beam. The experiment took place in June 2021. The left panel of Fig.5 shows a sketch of the experimental setup.

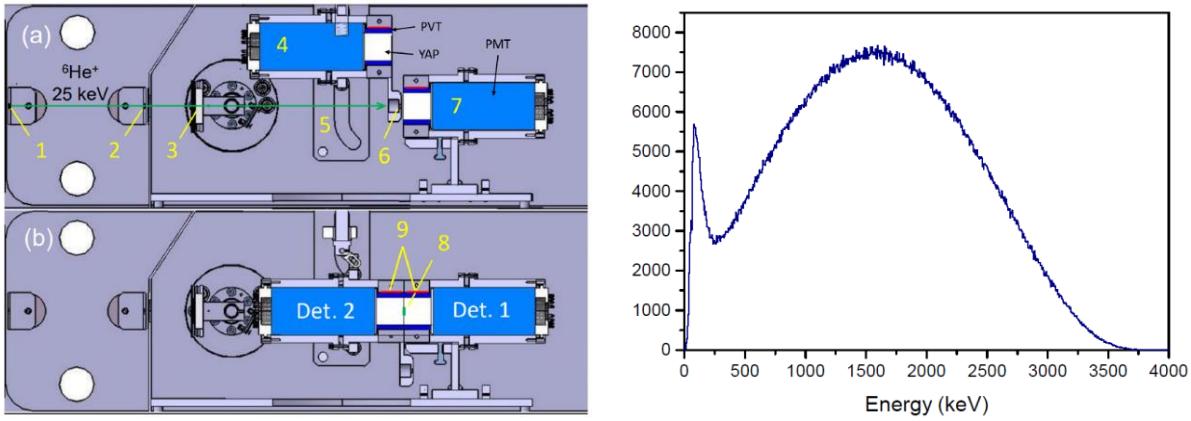


Fig.5. Left: sectional view of the setup at LIRAT showing the positions of detectors during beam implantation (a) and during data taking (b). The labels correspond to: 1 and 2— Ø6mm collimators; 3—movable Si detector; 4 and 5—moving YAP detector and guiding system; 6—Ø4mm collimator; 7—fixed YAP detector; 8—implantation region; 9—241Am sources. Right: typical experimental beta-energy spectrum obtained during a one hour run (from Ref. [Kan23a]).

The $^6$He$^+$ beam was produced by the SPIRAL target/ion-source system and was guided at 25 keV to the low energy beam line LIRAT at GANIL, after mass separation by a dipole magnet. The beam was chopped with a fast electrostatic deflector located upstream from the last dipole of the beam line in order to achieve the implantation/decay time sequence. The vacuum chamber is split in two sections with independent pumping systems [Fig.5 left panel (a)]. During beam tuning, a movable Si detector was inserted at the entrance of the detection section to measure the incoming beam intensity. The 4π solid angle coverage is achieved using two detectors. One of the detectors is fixed and aligned along the beam line whereas the other is mounted on a fast actuator. The $^6$He beam was implanted on the front face of the fixed detector at a mean depth of about 130 nm, while the moving detector is located out from the beam [Fig.5 left panel (a)]. In this configuration, the beam passes across a third Ø4 mm collimator located a few mm from the fixed detector surface. The time sequence consists of an implantation interval of typically 2.5 s, followed by a 1 s waiting interval during which the movable detector is brought in contact with the fixed detector [Fig.5, right panel, (b)], and finally a measuring interval of about 10-15 s. The front faces of both detectors are not covered by any light reflector. Part of the light produced in one detector is then detected by the other. The movable detector remains in the measuring position during data taking before being lifted up to start over a new cycle.

This closed geometry ensures the full collection of beta particles emitted by the implanted ions and prevents any partial energy loss due to backscattering. The duration of the data taking sequence was adjusted to be long enough such as to obtain a precise measurement of the ambient background. A 5 kBq $^{241}$Am source was permanently mounted on each detector to provide a constant calibration reference using the 59.54 keV photons. These interact mostly in the YAP volume whereas the 5 MeV alpha particles are stopped in the PVT which also serves as a veto to reject background events. The right panel in Fig.5 shows a typical energy spectrum taken during a run, after appropriate cuts and summing the energy from both detectors. The peak at about 100 keV is due to oversighting the shielding from Bremsstrahlung radiation produced by the beam implanted on the support of the last Ø4 mm collimator. The bottom cavity which is seen on the left panel of Fig.4, which was initially designed to position another radioactive source, was left open and the detectors were then unshielded against the radiation originating at the collimator. This can easily be improved in a future version of the setup. Measurements were carried out by blocking the beam at the level of the last collimator to clearly identify the background source, which was later well understood with Monte-Carlo simulations [Kan23a].

A number of systematic effects have been studied under the conditions of the experiment [Kan23b] all of which are about an order of magnitude smaller than the precision goal of Phase I. The data analysis is expected to be completed in 2024. The publication of the result will then constitute the major milestone of Step 1.

### 4.2 Phase I – Step 2: high energy experiment at LISE/GANIL

In a similar way, a critical turning point for Step 2 of Phase I was performing the experiment with the high energy beam. The experiment was carried out in April 2023. Figure 6 shows the main elements of the LISE beam line at GANIL for the production of a 52.7 MeV $^{6}He^{2+}$ beam. A 62.2 MeV/nucleon $^{13}C$ primary beam extracted from the GANIL coupled cyclotron system, was impinging on a 2 mm thick Be target. A 1 mm thick Be wedge shaped degrader was also used near the F31 slits for momentum selection. Several beam diagnostic elements were installed under vacuum, upstream of the final focal point in the D6 area. The $^{6}He^{2+}$ beam exited the beam line through a 50 µm thick Al foil. The YAP implantation detector was located in air (Fig.7, left panel). A plastic scintillator telescope located upstream from the YAP enabled detecting the ions from a possible beam halo outside a 1 cm$^2$ square aperture. Two sizes of YAP detectors were used in order to test and control the effect of Bremsstrahlung escape radiation.

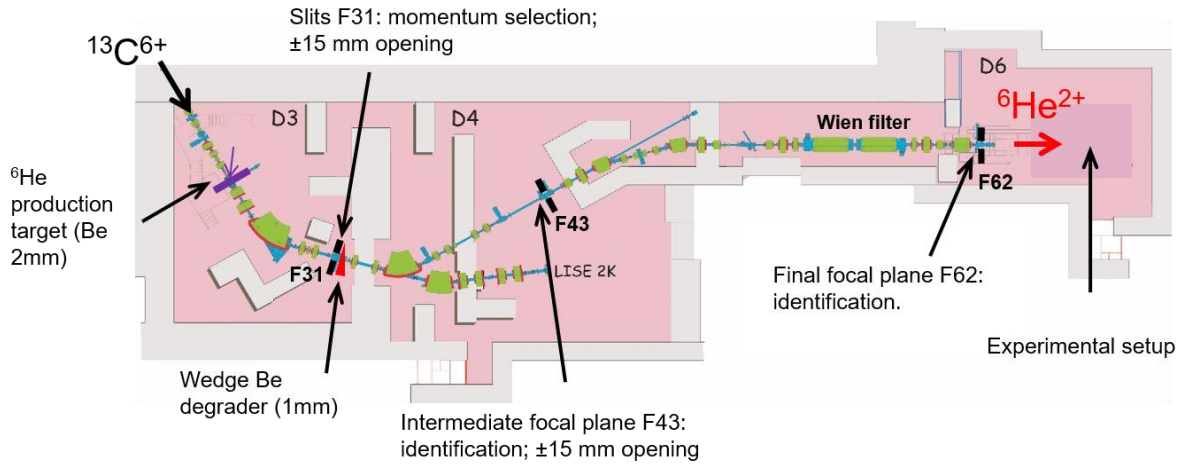


Fig. 6. Scheme of the LISE beamline at GANIL showing the main components for the production of a 52 MeV/nucleon $^{6}He^{2+}$ beam.

The right panel in Fig.7 shows a beta-energy spectrum recorded during a one hour run, after a crude calibration and background subtraction. The data analysis of the experiment performed at LISE is currently under way, and is the main topic of the PhD thesis of Romain Garreau at Université de Caen Normandie, which started in 2023. The results from Step 2 will be published and are also expected to be competitive compared to recent results in neutron and nuclear decays.

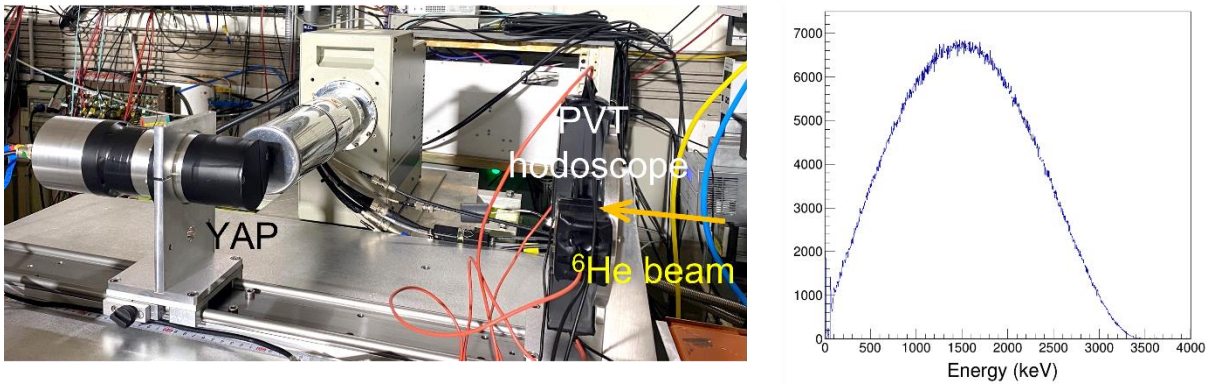


Fig.7. Left: picture of the experimental setup at LISE. The $^{6}$He beam comes from the right and goes in air through an open PVT hodoscope to be implanted in the YAP detector. Right: energy spectrum recorded during a one hour run by one of the YAP detectors.

### 4.2 Phase II

A critical comparison of pros and cons of the two methods from Step 1 and Step 2, will start in the fall 2024 based on actual conditions and results, along with the detailed analysis of data from Step 2. This should enable to assess possible improvements on the most promising technique, to engage into Phase II.

### 4.3 Bremsstrahlung escape characterization

As stated in Sec. 3.2 above, because of the finite size of the detectors, part of the Bremsstrahlung radiation produced by the beta particles during slowing down does escape the detector, producing a small distortion [Huy18]. This is not expected to be a limiting effect but, strictly speaking, no quantitative comparison is available for electrons in the energy range up to 4 MeV and for the material of the crystals used in the experiment (YAP). Also, the data available in the literature related to the Bremsstrahlung cross sections are not accurate enough for the purpose of the present measurement.

In order to benchmark the Geant4 predictions, dedicated measurements have been carried out in April 2024 at the Facility for Rare Isotope Beams at MSU, in collaboration with colleagues from Oak Ridge National Laboratory. The measurements used the Modular Total Absorption Spectrometer (MTAS) [Kar16] which has a very high efficiency for gamma-ray detection. Radioactive sources, in particular $^{90}$Sr, were located between two optically decoupled YAP detectors in a face-to-face geometry, similar to the one used for the low energy experiment [Fig.5, left panel (b)]. The full assembly was then inserted inside the open bore of MTAS [Kar16]. The beta particles were detected by the YAP scintillators whereas the escaping Bremsstrahlung radiation was detected by MTAS. This provides a well-defined and clean geometry for the comparison between the measurements and the predictions from Geant4 simulations.

### 4.4 Precise quantification of backscattering

In the setup used for the low-energy experiment [Fig.5, left panel, (b)] the two detectors are not optically isolated. It is then possible to precisely identify backscattering events for which the energy is shared between the two detectors. Figure 8 shows a 2D histogram of the energy deposited in one of the YAP detectors versus the energy deposited in the other, after correction for the light cross talk between the detectors [Kan23b].

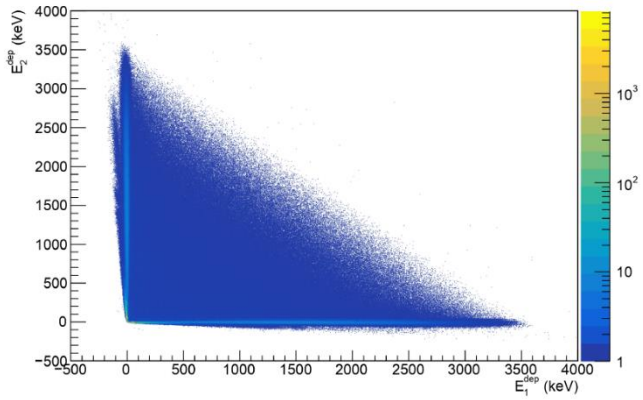


Fig.8. Two-dimensional histogram of the energy deposited in one of theYAP detectors versus the energy deposited in the other for the configuration of Fig.5 left (b), taken with an implanted $^6$He beam. Both energies were corrected for the light cross talk between the detectors.

Events for which one of the two energies is zero, correspond to beta particles fully detected by one of the two YAP modules. All other events correspond to backscattered beta particles with a partial energy deposition in each module. The analysis of this 2D plot will enable deducing precisely the backscattering fraction of electrons in YAP. Such information is not at all necessary for the analysis of the shape of the beta-energy spectrum but is a by product which will serve to test, and possibly improve, the Geant4 description of backscattering.

## 5 Positioning Relative to the International Competition

Several projects in neutron and nuclear decays, initially designed for measurements of other beta-decay correlations, have also reported new values of the Fierz interference term. This is due to the fact that almost all correlation coefficients, including those from integral measurements, become sensitive to the Fierz term [Gon16]. Recent results were mentioned and commented in Sec.2 above. We focus here on projects specifically developed for measurements of the beta-particle energy spectrum, using other techniques.

A new technique which has been proposed to eliminate the problem of backscattering, uses Cyclotron Radiation Electron Spectroscopy (CRES). The technique was initially developed within the Project-8 experiment, for the measurement of the neutrino mass in tritium decay, and was adapted for MeV beta particles. The measurement consists in the detection of the cyclotron frequency of the radiation emitted by beta particles in a magnetic field. A demonstrator which includes a cryo-cooler, low-noise amplifiers, RF-guides and a 7 T superconducting solenoid was built at University of Washington, Seattle. The proof of principle of the CRES technique applied to beta-particles from $^6$He and $^{18}$Ne decays, has recently been published [Byr23]. This is an elegant new approach which has still to address many challenges before a full measurement of the beta energy spectrum at the required level of precision could be achieved.

In comparison, the approach proposed in the *bSTILED* project has substantially less risks and is significantly less expensive. It is certainly also technically less innovative since it

uses rather standard techniques of precision spectroscopy, but this makes also its strength.

A recent preprint [Dek24] reports the use of a multi-wire drift chamber combined with a plastic scintillator for the measurement of the beta-energy spectrum in the $\beta^-$ decay of $^{114}$In. In the proposed setup, beta particles still undergo backscattering on the plastic scintillator and also on the wires and on the gas of the chamber. The collaboration reports a value for the Fierz term, $b_{GT} = 0.068(68)$. This is more than an order of magnitude larger than the current sensitivity level required from a single experiment [Gon19].

Another technique developed to reduce the effect of backscattering was also recently implemented in the Indium Energy Spectrum Shape (INESS) experiment [Van23]. The strong magnetic field of the setup used for the measurement of the beta-neutrino correlation in $^{32}$Ar [Ara20] confines the $\beta^-$ particle between two plastic scintillators located on both sides of an $^{114}$In source. Energy losses only arise from the dead layer of the radioactive source holder. This technique is somewhat similar the low-energy setup used in the *bSTILED* project but is difficult to adapt using radioactive ion beams online.

We consider that the *bSTILED* project maintains a fairly competitive position compared to similar dedicated projects.

# 6. Resources

## 6.1 Human resources

The IN2P3 laboratories involved in the project are the LPC Caen and GANIL. The LPC Caen is the main driver of the project whereas GANIL has provided the necessary resources to conduct the experiments. The two main scientists are X. Fléchard (LPC Caen) and O. Naviliat-Cuncic (formerly at LPC Caen and now at IRL Nuclear Physics and Nuclear Astrophysics and Michigan State University). Other personnel from LPC Caen involved in the project for specific tasks related to the preparation or running of experiments are J. Lory, D. Etasse, L. Hayen, F. Lebourgeois, E. Liénard, Ch. Vandamme, and J. Perronnel. One PhD thesis at Université de Caen Normandie has been funded by the Normandy Region (M. Kanafani) and one PhD thesis is currently being funded by IN2P3 (R. Garreau). At GANIL, the responsible scientists for the installation and running of experiments are S. Marie-Saillenfest, V. Morel and J.C. Thomas. The *bSTILED* collaboration also includes the LNHB of CEA. The beta spectrometry group at the LNHB is constituted by with two permanent staff (X. Mougeot and S. Leblond), working part-time on the project, and of a PhD student (Gaël Craveiro) who is involved in the experimental part of the *bSTILED* project. Internship student Thomas Gheereart was supported by the ANR contract to work on a data-acquisition system for the LNHB group.

## 6.2 Financial resources

The *bSTILED* ANR proposal, requested a total budget of 290 k€. About 40% of it was for the funding of a two-year post-doc position. The rest was for equipment, administration, operation and travel costs. No equipment funds have been requested to IN2P3 in the course of the project.

At the time of writing this report, it is difficult to project the evolution of future financial needs for equipment. Even assuming that at least one of the techniques will reach the expected level of sensitivity for Phase I, and that the planned comparative study will

foresee space for improvements to reach the goal of Phase II, we do not know at present what the modifications of the setups would be to make those improvements. However, faithfully to the style of the *bSTILED* project, in which relatively simple standard nuclear spectroscopy techniques have been implemented with the aim to compete with constraints obtained from LHC, we expect that possible modifications could be covered by the running ANR contract, as initially planned.

## 7. Technical Developments/Achievements

Although there have been a number of adaptions of spectroscopy tools and available techniques to perform the experiments described above, there were strictly no specific new technical development. We do not foresee any need in the future which could not be conceived and realized within the collaborating laboratories.

## 4. References


**[Ara20]** V. Araujo-Escalona et al., Phys. Rev. C **101** (2020) 055501

**[Bec24]** M. Beck, W. Heil, Ch. Schmidt, S. Baeßler, F. Glück, G. Konrad, and U. Schmidt, Phys. Rev. Lett. **132** (2024) 102501

**[Byr23]** W. Byron et al., Phys. Rev. Lett. **131** (2023) 082502

**[Bha12]** T. Bhattacharya, et al., Phys. Rev. D **85**. (2012) 054512.

**[Cir13]** V. Cirigliano, M.J. Ramsey-Musolf, Prog. Part. Nucl. Phys. **71** (2013) 2

**[Cra24]** G. Craveiro et al., Unfolding experimental distortions in beta spectrometry, submitted to Frontiers in Physics (2024)

**[Dek24]** L. De Keukeleere, D. Rozpedzik, N. Severijns, K. Bodek, L. Hayen, K. Lojek, M. Perkowski, S. Vanlangendonck, https://arxiv.org/abs/2404.03140

**[Fal21]** A. Falkowski, M. González-Alonso, O. Naviliat-Cuncic, J. High Energ. Phys. **2021** (2021) 126

**[Gel58]** M. Gell-Mann, Phys. Rev. **111** (1958) 362

**[Gol08]** V.V. Golovko, V.E. Iacob, J.C. Hardy, Nucl. Instrum. Methods Phys. Res. A **594** (2008) 266

**[Gon16]** M. González-Alonso, O. Naviliat-Cuncic, Phys. Rev. C **94** (2016) 035503

**[Gon19]** M. González-Alonso, O. Naviliat-Cuncic, N. Severijns, Prog. Part. Nucl. Phys. **104** (2019) 165

**[Har15]** J.C. Hardy, I.S. Towner, Phys. Rev. C **91** (2015) 025501.

**[Har20]** J.C. Hardy and I.S. Towner, Phys. Rev. C **102** (2020) 045501

**[Huy18]** X. Huyan, O. Naviliat-Cuncic. P. Voytas, S. Chandavar, M. Hughes, K. Minamisono, S.V. Paulauskas, Nucl. Instrum. Methods Phys. Res. A **879** (2018) 134

**[Hug19]** M. Hughes, PhD thesis, Michigan State University, 2019 (unpublished).

**[Huy19]** X. Huyan, PhD thesis, Michigan State University, ProQuest Dissertations Publishing, 2019, 22613979

**[Huy20]** X. Huyan, private communication 2020.

**[Kan22]** M. Kanafani, X. Fléchard, O. Naviliat-Cuncic, G.D. Chung, S. Leblond, E. Liénard, X. Mougeot, G. Quéméner, A. Simancas Di Filippo, J.C. Thomas, Phys. Rev. C **106** (2022) 045502

**[Kan23a]** M. Kanafani, X. Fléchard, O. Naviliat-Cuncic, G.D. Chung, S. Leblond, E. Liénard, X. Mougeot, G. Quéméner, A. Simancas Di Filippo, J.C. Thomas, EPJ Web of Conferences **282** (2023) 01010

**[Kan23b]** M. Kanafani, PhD thesis, Université de Caen Normandie, 2023; https://theses.hal.science/tel-04466399

**[Kar16]** M. Karny, K.P. Rykaczewski, A. Fijalkowska, B.C. Rasco, M. Wolińska-Cichocka, R.K. Grzywacz, K.C. Goetz, D. Miller, E.F. Zganjar, Nucl. Instrum. Methods Phys. Res. A **836** (2016) 83

**[Jac57]** J.D. Jackson, S.B. Treiman, H.W. Wyld Jr, Nucl. Phys. **4** (1957) 206

**[Lon24]** B. Longfellow et al., Phys. Rev. Lett. **132** (2024) 142502

**[Mar03]** J.W. Martin, J. Yuan, S.A. Hoedl, B.W. Filippone, D. Fong, T.M. Ito, E. Lin, B. Tipton, and A.R. Young, Phys. Rev. C **68** (2003) 055503

**[Mar06]** J.W. Martin, J. Yuan, M.J. Betancourt, B.W. Filippone, S.A. Hoedl, T.M. Ito, B. Plaster, and A.R. Young, Phys. Rev. C **73** (2006) 015501

**[Mos98]** M. Moszynski, et al., Nucl. Instrum. Methods Phys. Res. A **404** (1998) 157

**[Mou22]** $^{6}$He - Comments on evaluation of decay data, http://www.lnhb.fr/nuclides/He-6_com.pdf and Tables of $^{6}$He decay http://www.lnhb.fr/nuclides/He-6_tables.pdf

**[Mul22]** P. Müller et al., Phy. Rev. Lett. 129 (2022) 182502

**[Nav13]** O. Naviliat-Cuncic, M. Gonzalez-Alonso, Ann. Phys. (Berlin) **525** (2013) 600

**[Nav16]** O. Naviliat-Cuncic, AIP Conf. Proc. **1753** (2016) 060001

**[Pau23]** M. Paulsen et al., submitted to Phys. Rev. C, https://arxiv.org/pdf/2309.14014

**[Sau20]** H. Saul, C. Roick, H. Abele, H. Mest, M. Klopf, A. K. Petukhov, T. Soldner, X. Wang, D. Werder, and B. Märkisch, Phys. Rev. Lett. **125** (2020) 112501

**[Sin23]** A. Singh, X. Mougeot, S. Leblond, M. Loidl, B. Sabot, A. Nourreddine, Nucl. Instrum. Methods Phys. Res. A **1053** (2023) 168354

**[Sot13]** G. Soti, F. Wauters, M. Breitenfeldt, P. Finlay, I.S. Kraev, A. Knecht, T. Porobic, D. Zakoucky, N. Severijns, Nucl. Instrum. Methods Phys. Res. A **728** (2013) 11

**[Sun20]** X. Sun, et al., Phys. Rev. C **101** (2020) 035503

**[Van23]** S. Vanlangendonck, *The effect of weak magnetism on the shape of the $^{114}$In beta energy*, PhD thesis, KU Leuven (2023) (unpublished).

**[Vos15]** K.K. Vos, H.W. Wilschut, R.G.E. Timmermans, Rev. Mod. Phys. **87** (2015) 1483